Supporting Information for

Wettability Gradient Colorimetric Sensing by Amphiphilic Molecular Response

Wei Hong, Haoran Li, Xiaobin Hu, Binyuan Zhao, Fan Zhang*, Di Zhang* and *Zhou Xu*

State Key Lab of Metal Matrix Composites, School of Materials Science and Engineering, Shanghai Jiao Tong University, Shanghai 200240, China.

AUTHOR INFORMATION: hxb@sjtu.edu.cn (X. Hu), mtsmmc@sjtu.edu.cn (F. Zhang)

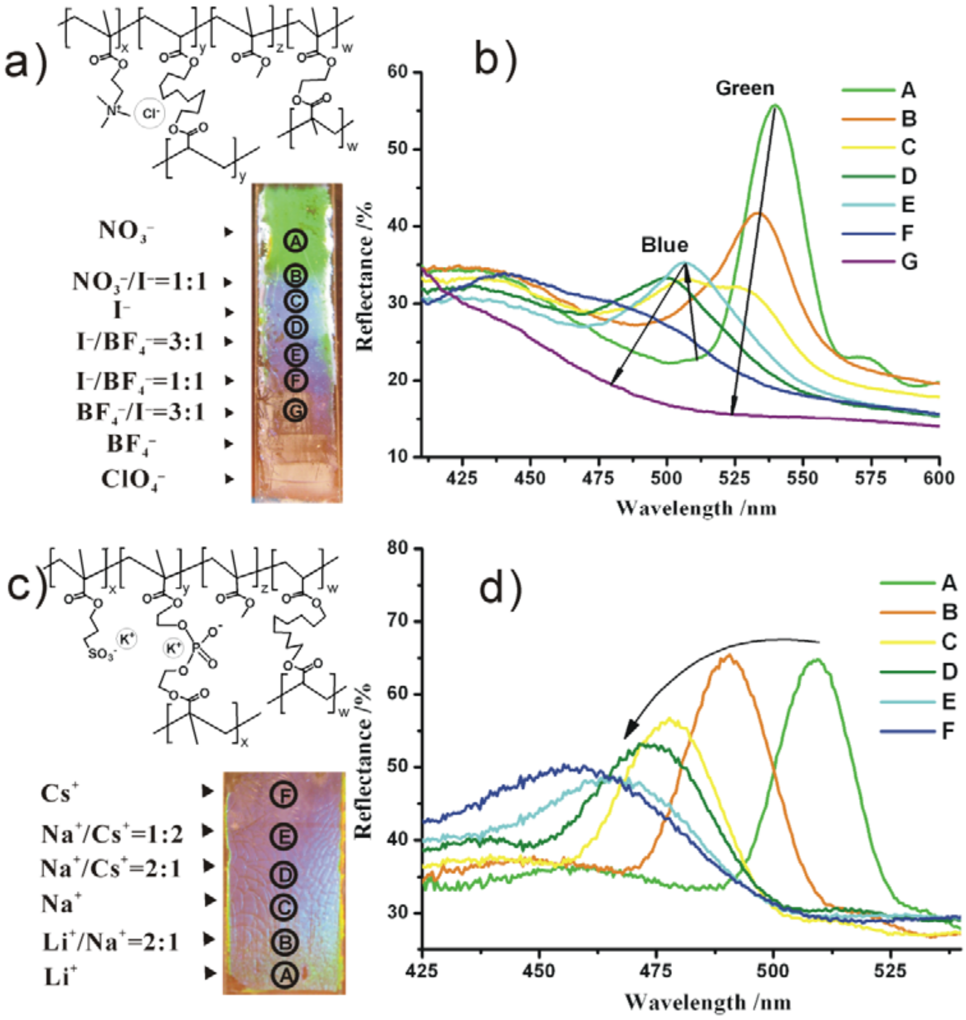

Figure S1. a) The copolymer structure of WGPF-A and the anion sequence used to create wettability gradient on it. b) Reflectance spectrum of the positions showed in Fig.S1a on WGPF-A. c) The copolymer structure of WGPF-C and the cation sequence used to create wettability gradient on it. d) Reflectance spectrum of the positions showed in Fig.S1c on WGPF-C.

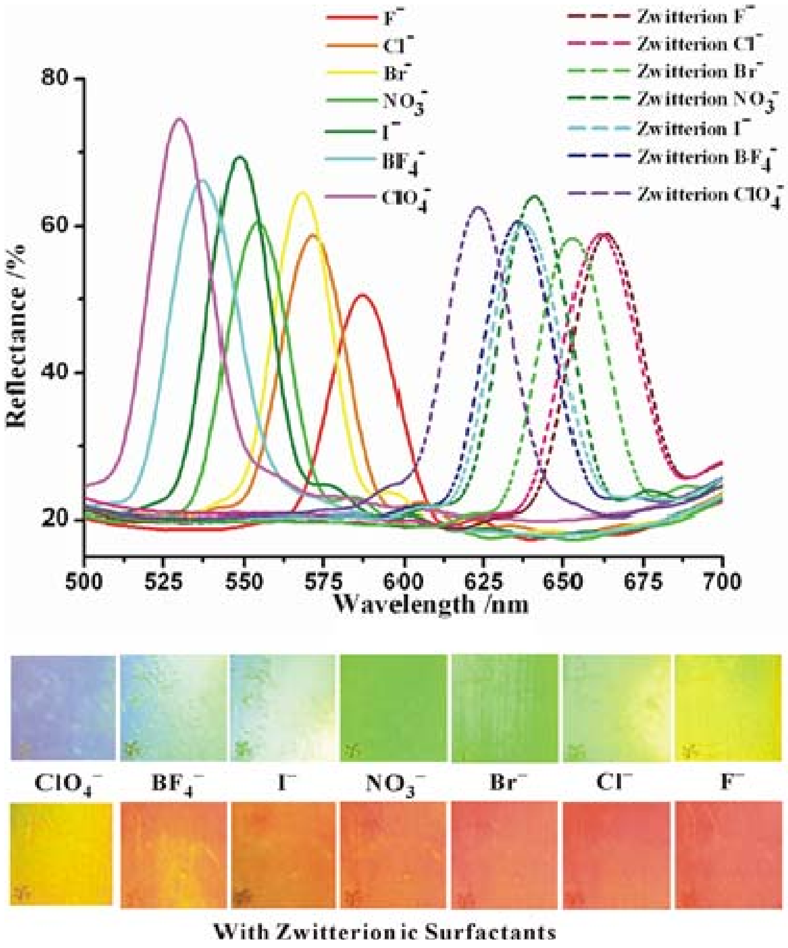

Figure S2. The reflectance spectrum and induced color change of PF-A (without wettability gradient) in 0.1 M diversified anion solutions before and after soaking in 5 mM myristyl sulfobetaine solution.

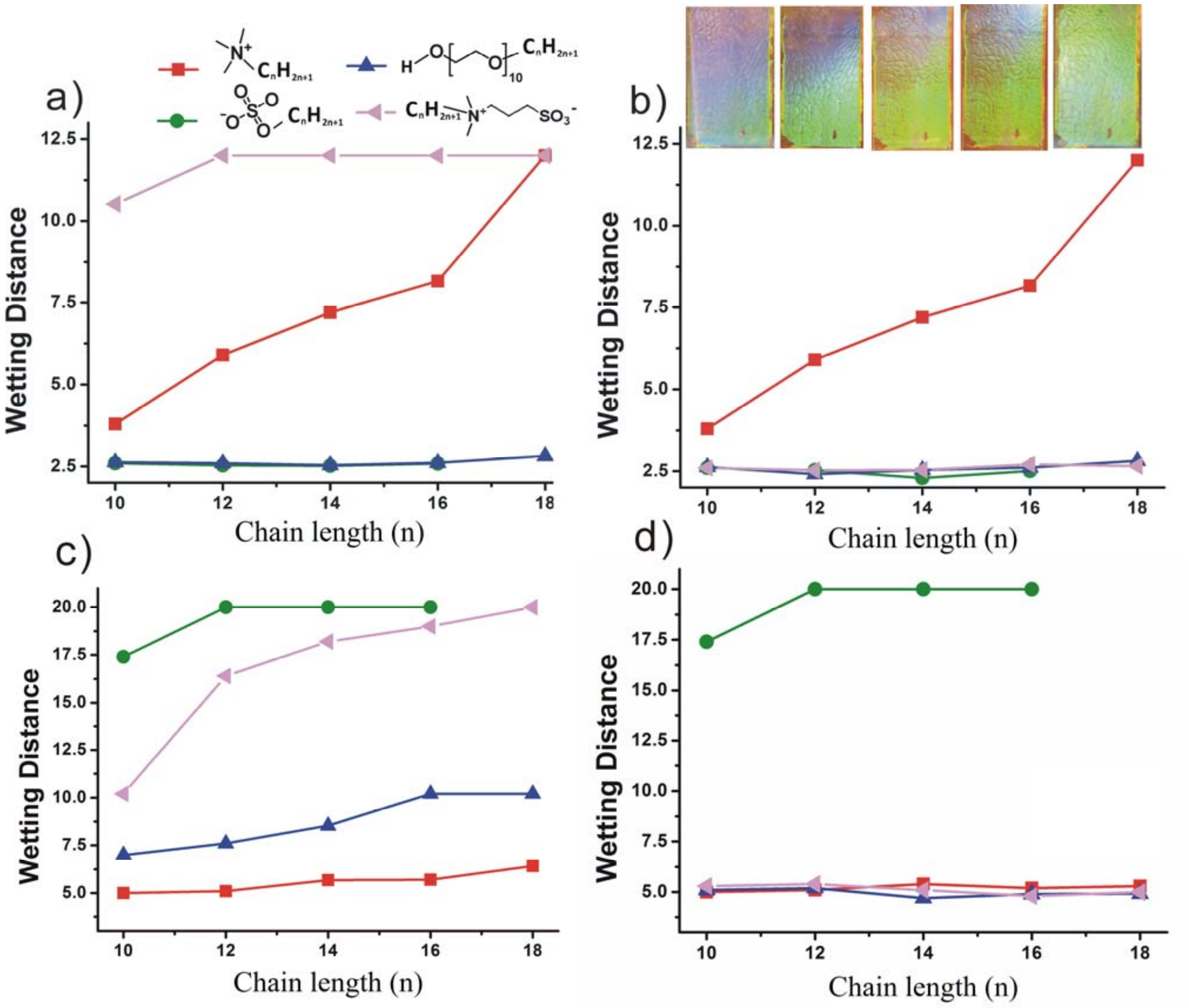

Figure S3. Effects of hydrocarbon chain of the surfactants (2 mM aqueous solution) on WGPFs at 298 K. The vertical ordinate “Wetting Distance” indicated the same as “Distance” in Fig.1b and d.

a) measured wetting distance after WGPF-C soaking in the solution. b) measured wetting distance of WGPF-C after the following process: 1. soaking the film in the surfactant solution; 2. washing the film by water/ethanol mixture for 15 minutes (removing the zwitterionic surfactants); 3.drying the film again and soaking it in water. The images showed the wetting degree of WGPF-C with the corresponding cationic surfactants after the process. c) measured wetting distance after WGPF-A soaking in the solution. d) measured wetting distance of WGPF-A after the process of Fig.S3b.

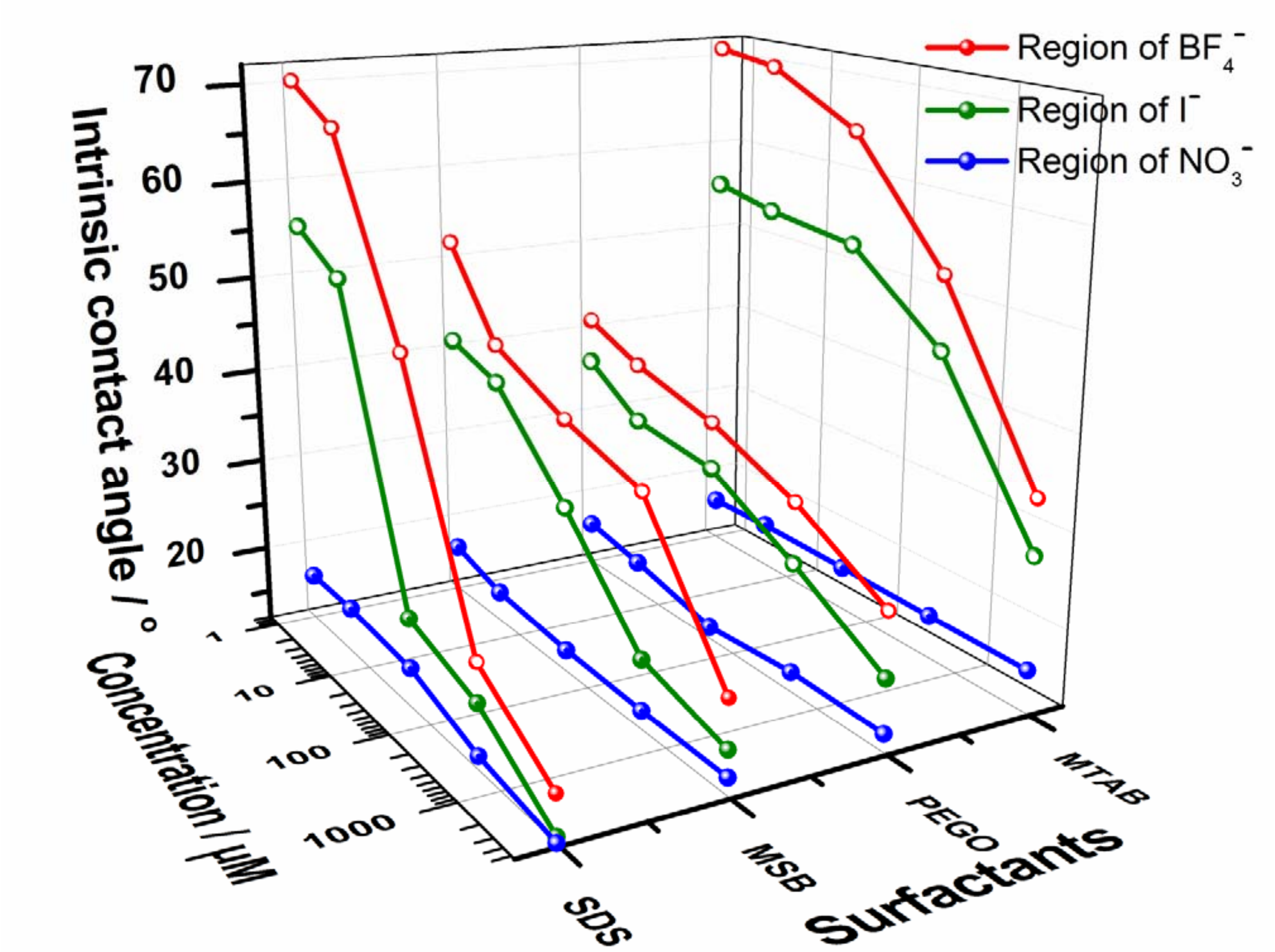

Figure S4. Measured contact angles from different surfactant concentrations in water on flat WGPF-A surfaces with counterions of NO_3^-, I^- and BF_4^-. Filled markers indicate the regions were infiltrated by the solution. SDS: sodium dodecyl sulfate. MSB: myristyl sulfobetaine. PEGO: polyethylene glycol monooleyl ether. MTAB: myristyltrimethylammonium bromide.

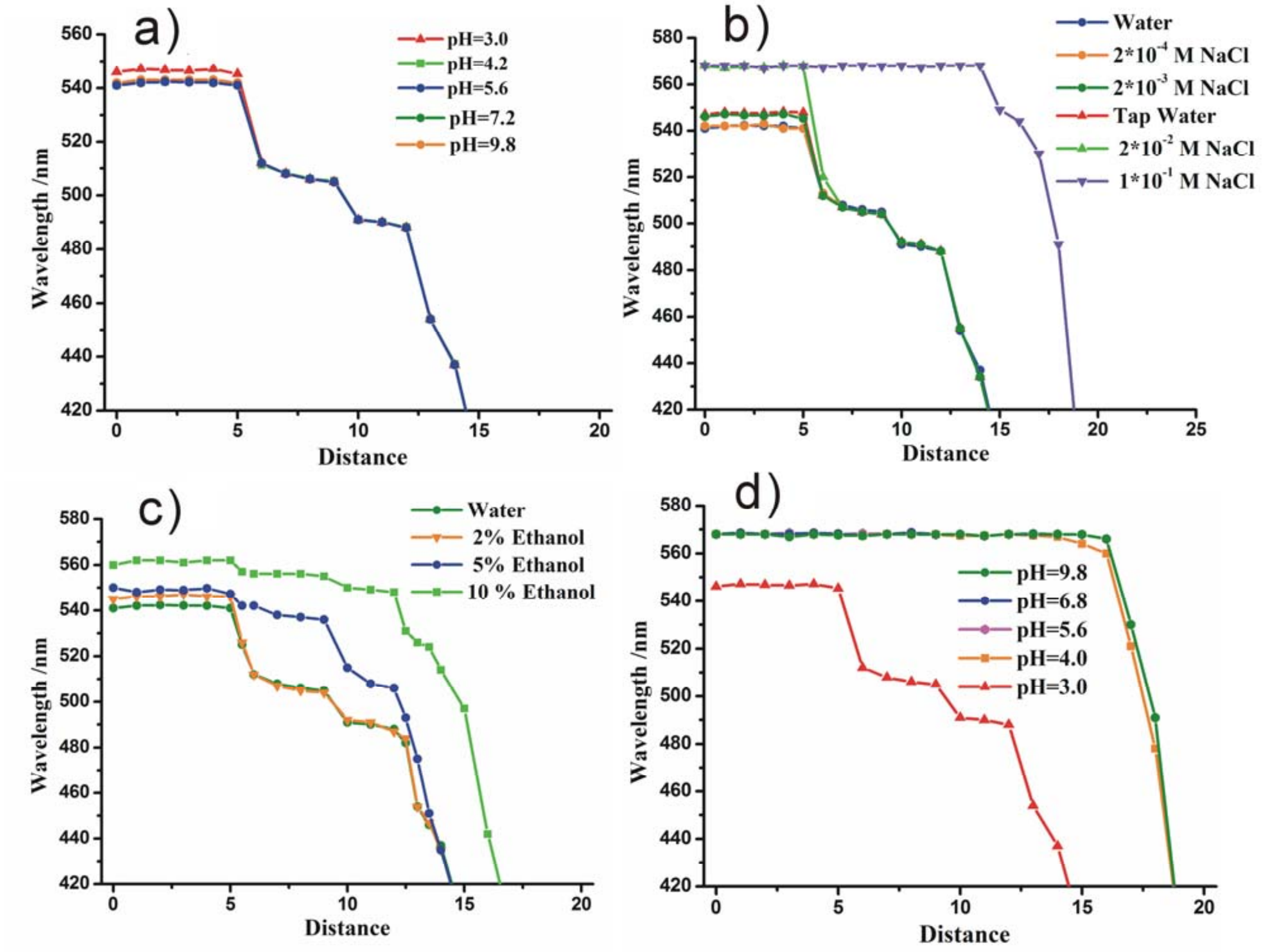

Figure S5. a) Effects of pH on the diffraction maximum distribution of WGPF-A.

b) Effects of ionic strength on the diffraction maximum distribution of WGPF-A.

c) Effects of ethanol (mixture with water) on the diffraction maximum distribution of WGPF-A.

The abscissa axis “Distance” means the same as Fig.1b.

d) Effects of pH on WGPF-A response to Gemini1. Gemini1 concentration: 10 µM. pH was adjusted by adding HCl and NaOH solution.

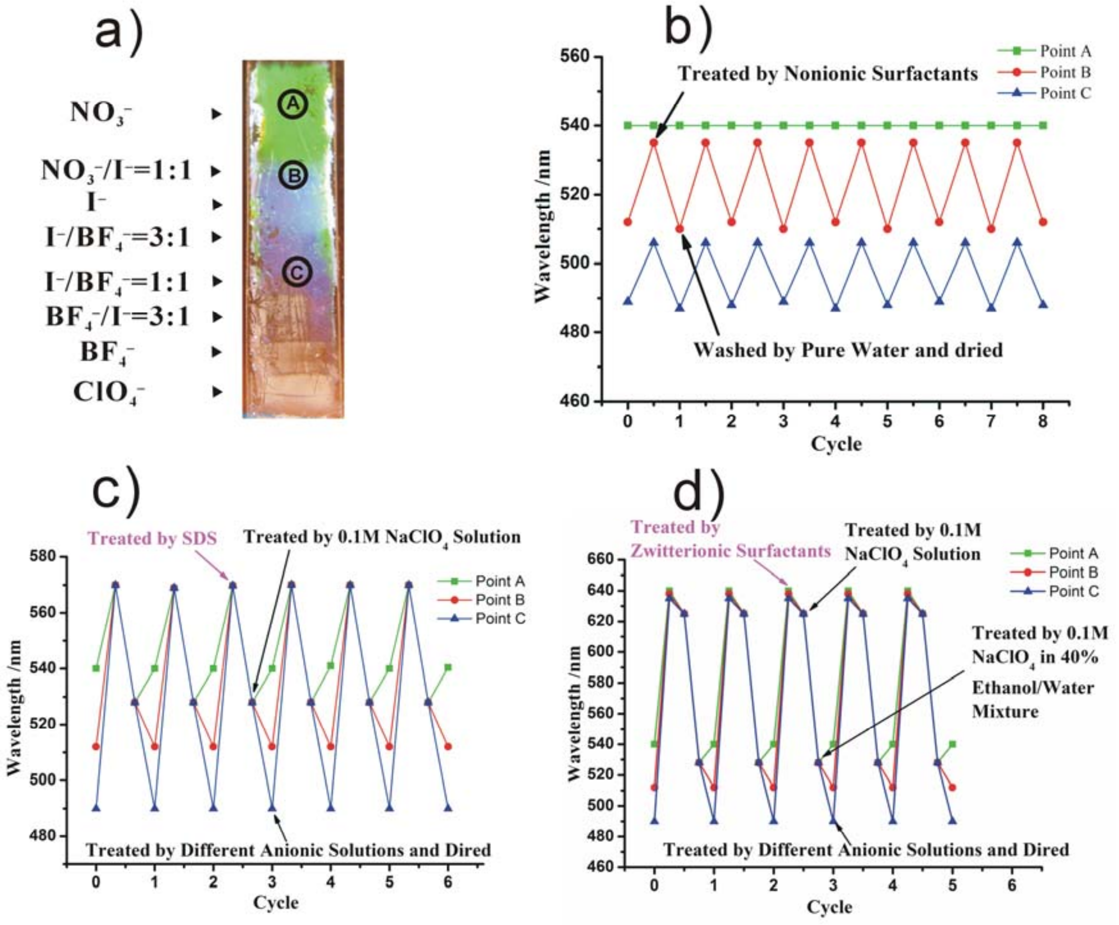

Figure S6. a) Image showing the position of A, B and C on WGPF-A in Figure S6.

b) Diffraction maximum of A, B and C recorded in 8 cycles of WGPF-A in nonionic surfactant response. One cycle included: 1.Immersed the WGPF-A in 5mM polyethylene glycol monooleyl ether solution; 2. Washed WGPF-A in water and dried it.

c) Diffraction maximum of A, B and C recorded in 6 cycles of WGPF-A in anionic surfactant (SDS) response. One cycle included: 1.Immersed the WGPF-A in 5mM SDS solution; 2. Washed WGPF-A in 0.1M $NaClO_4$ solution; 3. Treated the WGPF-A again by ion-exchange process showed in Scheme.1b and dried it.

d) Diffraction maximum of A, B and C recorded in 5 cycles of WGPF-A in zwitterionic surfactant response. One cycle included: 1.Immersed the WGPF-A in 5mM myristyl sulfobetaine solution; 2. Washed WGPF-A in 0.1M $NaClO_4$ solution; 3. Washed WGPF-A in 0.1M $NaClO_4$ in ethanol/water mixture; 4. Treated the WGPF-A again by ion-exchange process showed in Scheme.1b and dried it.

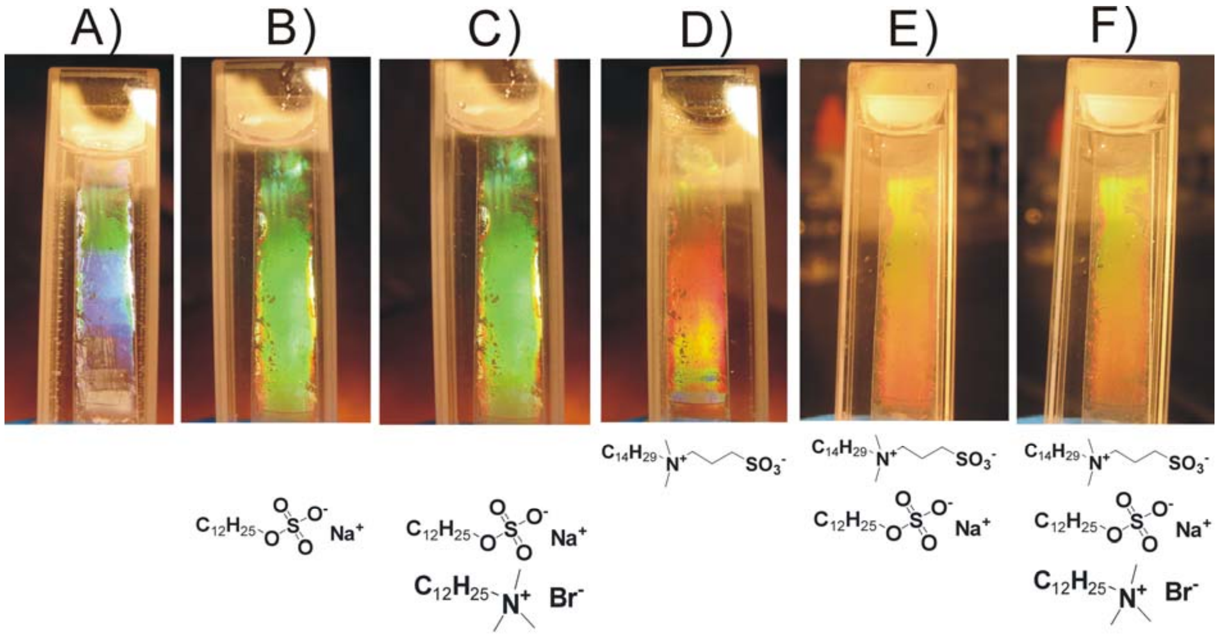

Figure S7. Detection of WGPF-A in competitive environment. Anionic, cationic and zwitterionic surfactants were mixed together in tap water. The concentration of each surfactant was 3mM.

A) WGPF-A in tap water.

B) Anionic surfactant only. WGPF-A showed completely wetting with green color.

C) Anionic surfactant mixed with cationic surfactants. WGPF-A showed completely wetting with green color, indicating that the cationic surfactant had little interference.

D) Zwitterionic surfactant only. WGPF-A showed partly wetting with red color.

E) Zwitterionic surfactant mixed with anionic surfactant. WGPF-A showed completely wetting with orange color.

F) Zwitterionic surfactant mixed with anionic surfactant and cationic surfactant. WGPF-A also showed completely wetting with orange color.

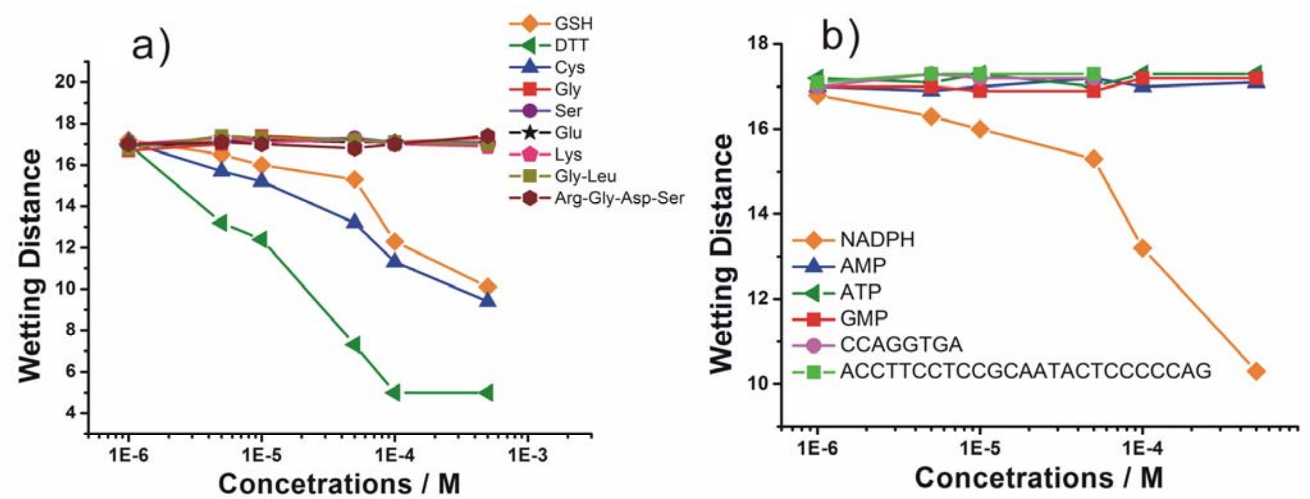

Figure S8. a) Effects of GSH, DTT and Cys concentrations on WGPF-A with the control group of amino acids and peptides. All the solutions contained 0.01 mM Gemini1 at pH=6.5. The vertical ordinate "Wetting Distance" indicated the same as "Distance" in Fig.1b. b) Effects of NADPH concentrations on WGPF-A with the control group of AMP, ATP, GMP and two DNA sequence. All the solutions contained: 0.01 mM Gemini2, 2 mM pH=7.4 phosphate buffer with glutathione reductase, and 0.05 mM GSSG. The concentration of the DNA sequence was based on the nucleotide concentration. The vertical ordinate "Wetting Distance" indicated the same as "Distance" in Fig.1b.

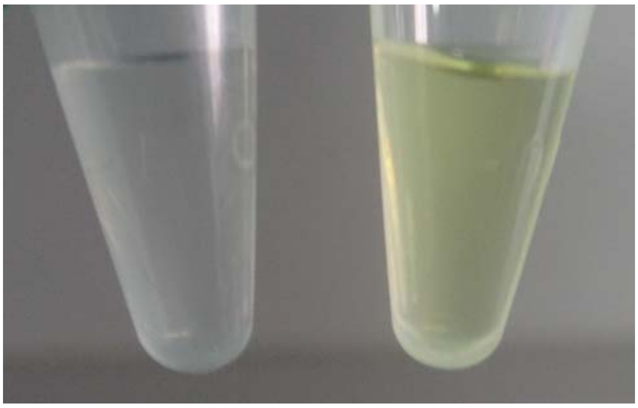

Figure S9. Activity test of glutathione reductase by DTNB method [4].

(Left) The inhibition of the glutathione reductase by GSSG based gemini surfactant.

(Right) No significant inhibition by cystine based gemini surfactant.

Substrate concentrations: GSSG=5*10^{-5}M, NADPH=5*10^{-5}M, Gemini1(left) =1*10^{-5}M and Gemini2(right)=1*10^{-5}M, DTNB (dissolved in DMSO) = 2*10^{-5}M, pH=7.4 at room temperature.

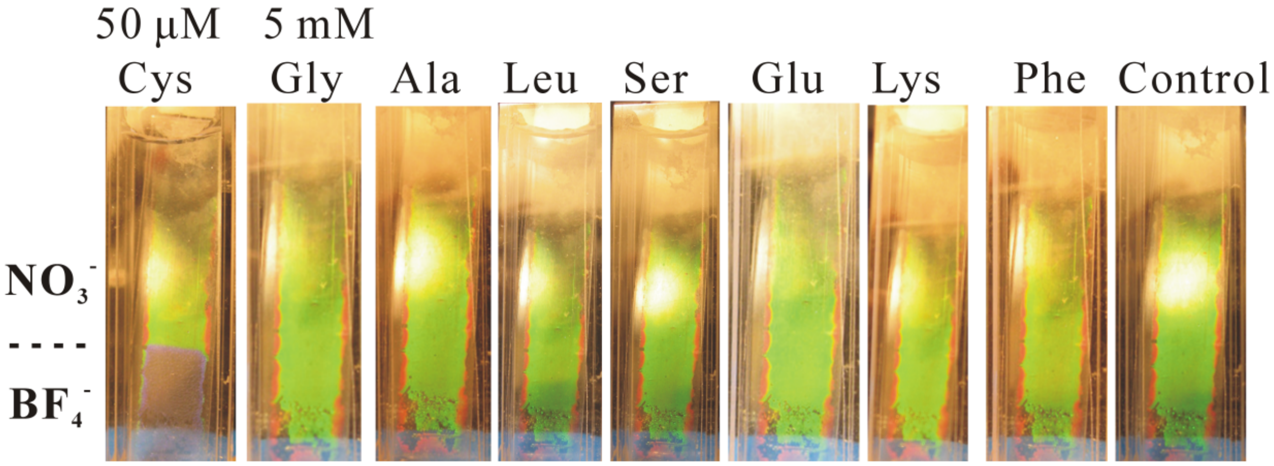

Figure S10. Concise sensing by the most sensitive region. Since the most sensitive region of Cys detection in Fig.2 was the BF_4^- region, the film was treated with two counter-ions: NO_3^- and BF_4^-. Different amino acids were mixed with 10 μM Gemini1. The concentration of Cys was 50 μM and other amino acids were 5mM.

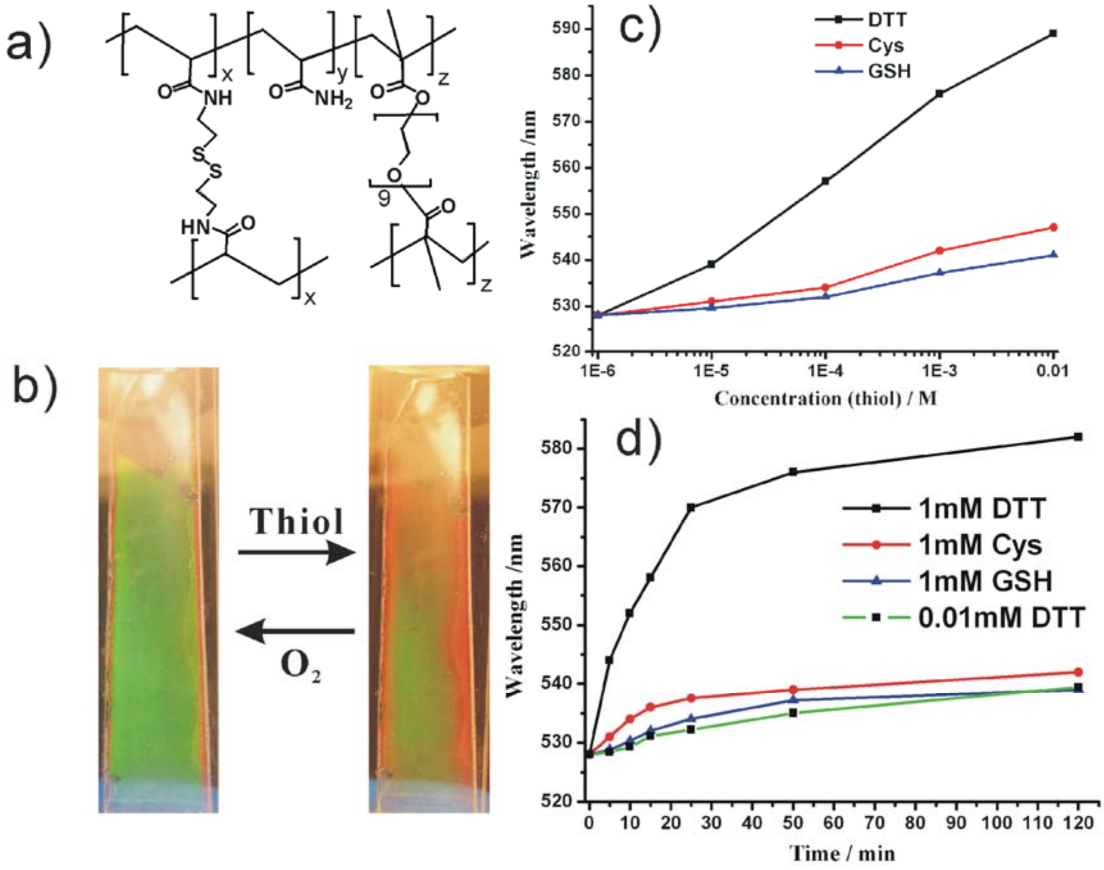

Figure S11. The prepared N,N'-bis(acryloyl)cystamine crosslinked inverse opal hydrogel for comparison with the gemini-assisted detection method. As the figure showed, such inverse opal hydrogel had about 10 nm shift for maximum response to Cys and GSH with long equilibrium time over 120 minutes.

a) Copolymer structure of N,N'-bis(acryloyl)cystamine crosslinked photonic hydrogel.

b) Images showing the color response of thiols and oxidants.

c) Reflectance spectrum of the photonic film showing the reduction effect of DTT, Cys and GSH on the N,N'-bis(acryloyl)cystamine crosslinked photonic films.

d) Responding time of the N,N'-bis(acryloyl)cystamine crosslinked photonic films.

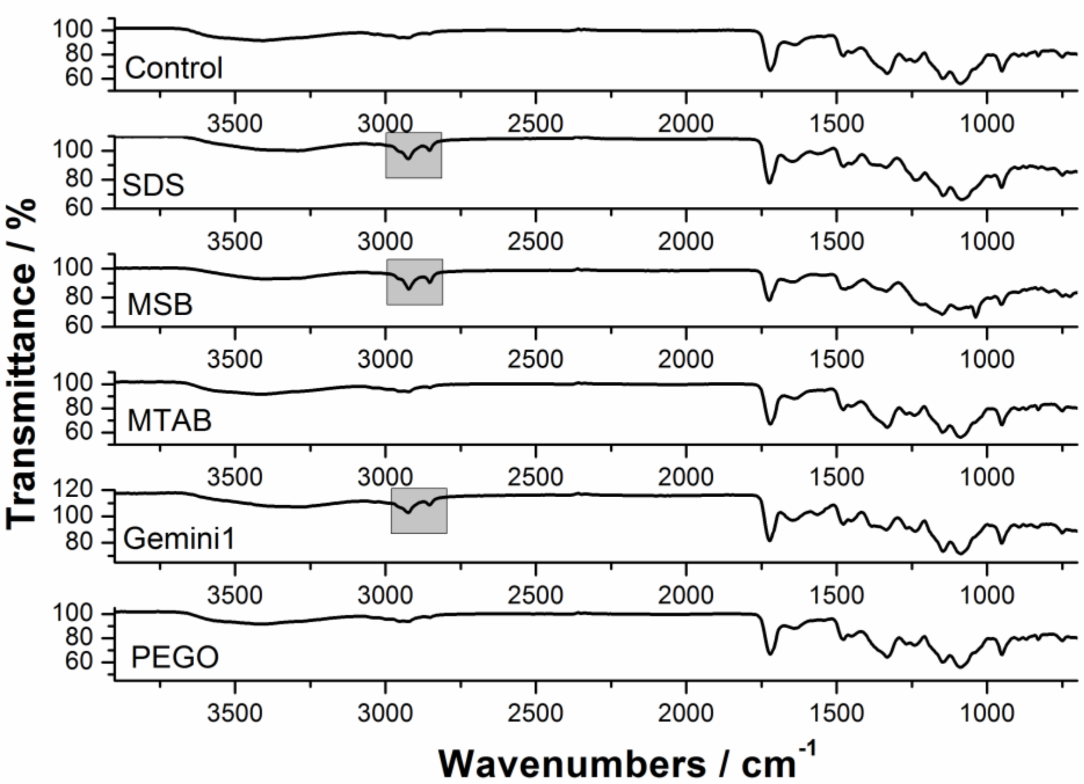

Figure S12. Micro-FTIR on WGPF-A. “Control” indicates WGPF-A with NO_3^- as counter-ion. The film was immersed into different surfactant solutions in 5 mM (Gemini1 in 10 μM) for 1 minute. After that, the film was washed by pure water for three times, then dried and went for Micro-FTIR. Absorption (or counter-ion exchange) of SDS, MSB and Gemini1 were evidenced by the significant enhanced 2922cm^{-1} and 2852 cm^{-1} signal from -CH_2- antisymmetric stretching vibration and symmetrical stretching vibration.

Table.S1 Element analyze of WGPF-A after surfactant response.

Sample	**N content / %**	**C content / %**	**S content / %**	**N%:C%**
Control	4.98	47.04	Not detected	0.106
SDS	3.00	49.81	2.26	0.060
MSB	3.63	43.45	1.21	0.084
PEGO	4.70	46.05	Not detected	0.102
MTAB	3.19	43.07	Not detected	0.074

"Control" indicates WGPF-A with NO_3^- as counter-ion. The film was immersed into 5mM different surfactant solutions overnight, then rinsed with plenty of water and dried for analyze (the quality of each sample was about 5 mg). Since SDS exchanged the NO_3^-, the N% dropped significantly and S% increased. MSB was absorbed into the film without ion-exchange, so that the N% dropped not so significantly and S% also increased. PEGO led to no obvious changes. The N% change caused by MTAB was caused by the counter-ion exchange for Br^-.

Table.S2 CMC value of different surfactants in this work and the corresponding response of WGPF-A according to Fig.1, Fig.2 and Fig.S3.

Surfactants	MSB		MTAB		PEGO		SDS		Gemini1	
CMC / μM	320[5]		2100		~1		8000		~50	
Concentration / μM	500	5000	500	5000	500	5000	10	500	5000	10
Wetting Distance (Max: 20 Min: 5.0)	5.0	5.0	12.8	17.5	5.0	9.8	5.0	14.6	20	17.5

Explanation of Scheme 1c:

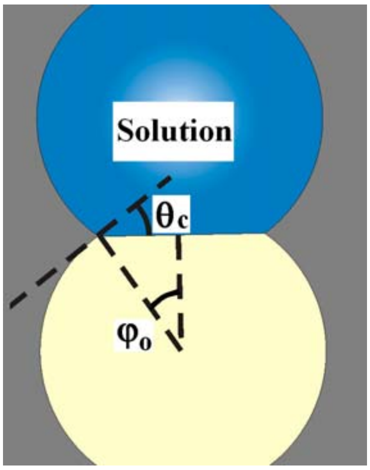

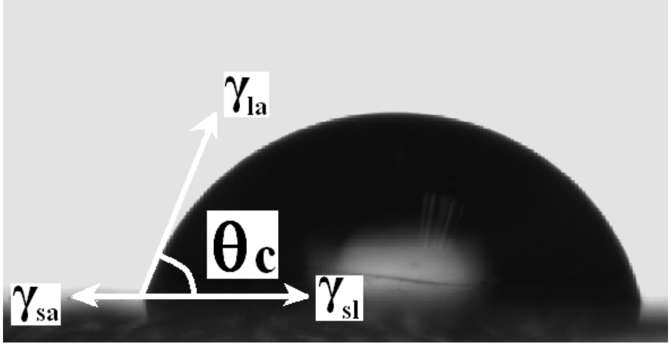

Inverse opal structure is simplified as a calabash-like model with two pores. The pore size is approximately considered to be fixed, because in our system the diffraction maximum shift was only estimated as 4%, from I^- and NO_3^- (about 550 nm) to SDS, Gemini1 and Gemini2 (about 570 nm), so that the effect from the swelling was limited.

Then $\Delta \mathrm{G} = \gamma_{\mathrm{la}} \pi R^2 \{(\sin\varphi)^2 - (\sin\varphi_0)^2] - 2(\cos\theta_{\mathrm{c}})(\cos\varphi_0 - \cos\varphi)\}$, which is the formula outlined by reference 11a. Based on this formula, there could be a energy barrier when $\theta_{\mathrm{c}} > \varphi_0$:

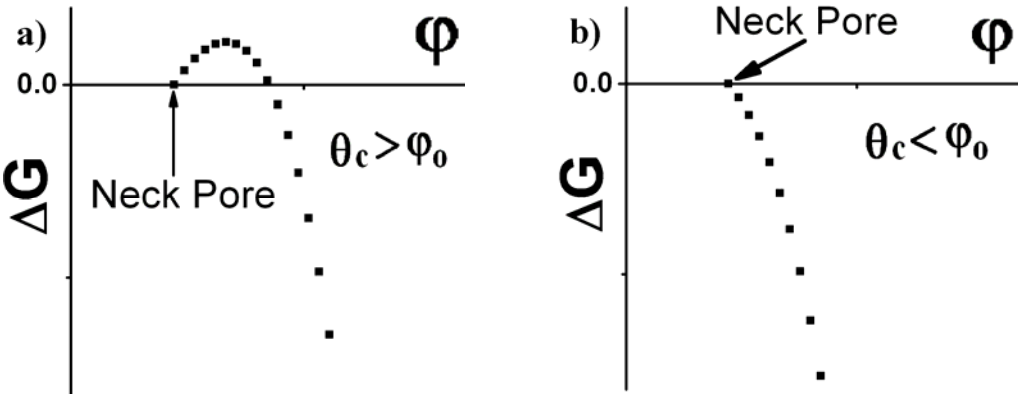

Scheme S1. a) When $\theta_{\mathrm{c}} > \varphi_0$, the change of Gibbs free energy with the increase of φ .

b) When $\theta_{\mathrm{c}} < \varphi_0$, the the change of Gibbs free energy with the increase of φ .

In this work, the φ_0 was about 22^{o} from the SEM image, so that as Fig.S4 showed, the critical θ_c was about 22^{o} .

Experimental section

Synthesis of monodisperse latex silica spheres: Monodisperse silica spheres and silica PC templates were obtained via previously reported method.[1]

Preparation of ion-exchangeable inverse opal films: Inverse opal films were fabricated using PC template method. Firstly, a PMMA slice was covered onto the glass slide with silica PC. After the infiltration of homogeneous monomer precursor into the gap between the two slices, polymerization was carried out under an ultraviolet lamp. The prepared inverse opal films could directly adhere onto the PMMA slice. Finally, the silica PC templates were removed by 1.2 % hydrofluoric acid, leaving the inverse opal films.

Creating wettability gradient on the inverse opal films: The obtained inverse opal films were dried and vertically positioned in a 0.1 M (anion or cation) solution with the highest liquid level. After the ion-exchange, the films were washed by pure water, dried, and then vertically positioned in the next solution with a lower liquid level. Such process repeated several times (see Scheme 1b). The composition and sequence of the solutions could refer to Fig.S1. Finally the wettability gradient inverse opal films (WGPFs) were washed by pure water and dried before used.

Surfactant-sensitivity of WGPFs: In order to evaluate the surfactant-sensitivity of the prepared WGPF, different surfactants were dissolved in pure water and the WGPFs were immersed into the solutions for 2-3 minutes to ensure the equilibrium. (For small molecule thiols and NADPH detection, it needed about 30 minutes to ensure the gemini-thiol reaction was complete.) After the WGPFs reached equilibrium, they were set into a microscope with positioning function for spectra of different positions on the films.

Characterization: The SEM pictures of the colloidal crystals and inverse opal films were obtained from a FEISirion200 SEM with an accelerating voltage of 5 kV. Before imaging, the samples were arc-coated with a thin gold film. The contact angles were measured on dataphysics Germany OCA20 contact-angle system. An average contact angle value was obtained by measuring the same sample at five different positions. The evaluation of the optical characteristics was obtained by Ocean Optic Maya

2000 fiber optic spectrometer combining a microscope with positioning function. All reflectance spectra were measured at near-normal incidence to the (111) planes. Images of the photonic films were recorded by a common digital camera under an incandescent lamp. Micro-FTIR was directly measured on the WGPF-A surface by Nicolet iN10 MX infrared imaging microscope (attenuated total reflection model). Element analyze was taken by Vario-ELIII IRMS element analyzer.

Formula of homogeneous monomer precursor for WGPFs:

WGPF-A: 160ul 80%DMC aqueous solution (0.68mmol), 105ul MMA (0.99mmol), 36ul EGDMA (0.19mmol), 45ul 1,9-bis(acryloyloxy)nonane (0.17mmol) and 1ul HMPP were mixed in a mixing solvent of 230ul acetic acid, 60ul water and 20ul ethanol.

WGPF-C: 50mg PSM (0.2mmol), 105ul MMA (0.99mmol), 64.4mg bis-[(2-methacryloyloxy)-ethyl]-phosphate (0.2mmol), 60ul 1,9-bis(acryloyloxy)nonane (0.22mmol) and 1ul HMPP were mixed in a mixing solvent of 200ul acetic acid, 60ul water and 30ul ethanol.

Formula of homogeneous monomer precursor for the N,N'-bis(acryloyl)cystamine crosslinked photonic hydrogel (the PMMA substrate should be firstly treated to have a PMMA inverse opal surface, and then the second layer of N,N'-bis(acryloyl)cystamine crosslinked photonic hydrogel could adhere to the PMMA substrate):

65mg N,N'-Bis(acryloyl)cystamine (0.25mmol), 178mg acrylamide (2.5mmol), 25ul PEG400-DMA (0.05mmol) and 1ul HMPP were mixed in 300ul acetic acid.

Preparation of GSSG based gemini surfactant (Gemini1):

GSSG based gemini surfactant (N,N'-bis-myristoyl-oxidized-L-glutathione) was synthesised by a previously reported method [2,3]. GSSG was reacted with myristoyl chloride in alkalic aqueous solution (pH=10-11) at 298K for 3h. Typically, to a solution prepared from 2.35 g (3.8 mmole) of oxidized L-glutathione in 60 ml of water and 0.614 g of sodium hydroxide, 2.4 ml (8.4 mmole) of stearoyl chloride was added with stirring over a period of 1h, and sodium hydroxide in 10 ml of water was added dropwise to maintain pH 10-11 at the same time. The reaction mixture was stirred two additional hours, cooled, diluted by 100ml water of 353K, and acidified to pH 3.5 with sulfuric acid to removed fatty acid and further acidified to pH 1 for final precipitation. The precipitated crude crystals of N,N'-bis-myristoyl-oxidized-L-glutathione were washed in petroleum benzine to obtain the pure crystals.

Preparation of cystine based gemini surfactant (Gemini2):

Cystine based gemini surfactant (N,N'-bis-myristoyl-L-cystine) was synthesized by the previously reported method of reference [2], similarly to the GSSG based gemini surfactant.

References:

[1] W. Hong, X. Hu, B. Zhao, F. Zhang, D. Zhang, **Tunable Photonic Polyelectrolyte Colorimetric Sensing for Anions, Cations and Zwitterions.** *Adv. Mater.* 2010, **22**, 5043.

[2] Y. Okahata, T. Seki, **pH-Sensitive Capsule Membranes. Reversible Permeability Control from the Dissociative Bilayer-Coated Capsule Membrane by an Ambient pH Change.**
J. Am. Chem. Soc. 1984, **106**, 8065.

[3] C. Gao, Y. Sakamoto, K. Sakamoto, O. Terasaki, S. Che, **Synthesis and Characterization of Mesoporous Silica AMS-10 with a Novel Bicontinuous Cubic Pn 3m Symmetry.** *Angew. Chem. Int. Ed.* 2006, **45**, 4295.

[4] G. Zhao, C. Yao-Yue, Gu. Qin, Li. Guo. **Luteolin from Purple Perilla mitigates ROS insult particularly in primary neurons.** *Neurobiol Aging.* 2012, **33**, 176.

[5] J. Zajac, C. Chorro, M. Lindheimer, and S. Partyka. **Thermodynamics of Micellization and Adsorption of Zwitterionic Surfactants in Aqueous Media.** *Langmuir* 1997, **13**, 1486.